Meteoritics & Planetary Science 39, Nr 7, 1233–1247 (2004)
Abstract available online at http://meteoritics.org

Evidence for ocean water invasion into the Chicxulub crater at the Cretaceous/Tertiary boundary

Kazuhisa GOTO,[1*] Ryuji TADA,[1] Eiichi TAJIKA,[1] Timothy J. BRALOWER,[2] Takashi HASEGAWA,[3] and Takafumi MATSUI[4]

[1]Department of Earth and Planetary Science, The University of Tokyo, Building #5, 7–3–1 Hongo, Tokyo 113–0033, Japan
[2]Department of Geosciences, Pennsylvania State University, 503 Deike Building, University Park, Pennsylvania 16802, USA
[3]Department of Earth Sciences, Kanazawa University, Kakuma-machi, Kanazawa 920–1192, Japan
[4]Department of Complexity Science and Engineering, The University of Tokyo, 7–3–1 Hongo, Tokyo 113–0033, Japan
[*]Corresponding author. E-mail: goto@eps.s.u-tokyo.ac.jp

(Received 29 August 2003; revision accepted 2 March 2004)

Abstract–The possibility of ocean water invasion into the Chicxulub crater following the impact at the Cretaceous/Tertiary boundary was investigated based on examination of an impactite between approximately 794.63 and 894.94 m in the Yaxcopoil-1 (Yax-1) core. The presence of cross lamination in the uppermost part of the impactite suggests the influence of an ocean current at least during the sedimentation of this interval. Abundant occurrence of nannofossils of late Campanian to early Maastrichtian age in the matrices of samples from the upper part of the impactite suggests that the carbonate sediments deposited on the inner rim margin and outside the crater were eroded and transported into the crater most likely by ocean water that invaded the crater after its formation. The maximum grain size of limestone lithics and vesicular melt fragments, and grain and bulk chemical compositions show a cyclic variation in the upper part of the impactite. The upward fining grain size and the absence of erosional contact at the base of each cycle suggest that the sediments were derived from resuspension of units elsewhere in the crater, most likely by high energy currents association with ocean water invasion.

INTRODUCTION

High-energy Cretaceous/Tertiary (K/T) boundary deposits have been reported at numerous locations near the impact site at Chicxulub. Some of these deposits are interpreted as resulting from tsunami (e.g., Bourgeois et al. 1988; Smit et al. 1996; Smit 1999). Recently, tsunami deposits were discovered at the K/T boundary in western Cuba, suggesting that the tsunami were of significant scale to have affected sedimentation in the deep proto-Caribbean Sea (Takayama et al. 2000; Tada et al. 2002, Forthcoming). However, the origin, magnitude, and extent of tsunami associated with the K/T boundary impact have not been determined in detail.

Matsui et al. (2002) proposed that ocean water invasion into the Chicxulub crater and subsequent overflow of ocean water from the crater was one of the possible mechanisms to generate a giant tsunami at the K/T boundary impact. Generation of tsunami by ocean water invasion has been postulated for other craters on the ocean floor (e.g., Lindström et al. 1994; Ormö and Lindström 2000; Dalwigk and Ormö 2001; Poag et al. 2002). However, ocean water invasion into the crater immediately after the impact and consequent generation of the tsunami at the K/T boundary has been questioned (e.g., Ormö and Lindström 2000) because water depth around the impact site was shallow (Sharpton et al. 1996; Pierazzo and Crawford 1997; Pierazzo et al. 1998), and because the crater rim may have prevented ocean water invasion into the crater. However, collapse of the crater rim was reported from the analysis of drilling cores recovered from the inside and outside the crater (Sharpton et al. 1996) and seismic reflection data (Morgan et al. 1997). Furthermore, according to numerical simulations, the transient crater rim collapsed within several minutes of the impact (Morgan et al. 2000; Collins et al. 2002), suggesting that ocean water invasion may have occurred rapidly.

If ocean water invaded the crater immediately after the impact, sedimentation of the impactite, defined as the variety of rocks produced during an impact event (e.g., French 1998), within the Chicxulub crater should have been influenced by an ocean current. However, a detailed analysis of the impactite within the Chicxulub crater has not been conducted because drilling core samples had not previously been available for high-resolution analyses.

In 2001 and 2002, the Chicxulub Scientific Drilling

Program (CSDP) sponsored by the International Continental Scientific Drilling Program (ICDP) and Universidad Nacional Autónoma de México (UNAM) cored the impactite within the Chicxulub crater. The drill hole, Yaxcopoil-1 (Yax-1), was situated approximately 65 km south of the crater center on the southern inside slope of the crater rim (Fig. 1) and a drilling core approximately 1500 m in length was recovered (Fig. 2).

In this study, we focused on the deposition of the uppermost part of the impactite in Yax-1 (794.63–808.02 m of sub-bottom depth) to explore whether ocean water invaded the crater immediately after the impact. This interval was deposited during the latest stage of the formation of the Chicxulub crater and, thus, is the most likely interval to contain evidence of ocean water invasion. The investigation integrated quantitative analyses of grain composition, chemical composition, maximum grain size, and nannofossil and planktonic foraminiferal assemblages.

STRATIGRAPHY

The recovered Yax-1 core consists of (from bottom to top): ~600 m-thick shallow water carbonate and sulfate rocks, ~100 m-thick impactite, and ~800 m-thick Tertiary carbonates (Fig. 2). The shallow water carbonate and sulfate rocks are thought to be mega-blocks of probable Cretaceous age deposited in association with the K/T boundary impact event based on the presence of shocked quartz, melt fragments, and impact melt dikes in intervals at 910 m, 916 m, and 1347 m (Kenkmann et al. 2003; Wittmann et al. 2003). The impactite is composed of an impact melt breccia and a suevite (Dressler et al. 2003a). The impact melt breccia is defined as a deposit composed of melt and rock fragments with a matrix of melt, while suevite is a deposit composed of melt and rock fragments with a clastic matrix (e.g., French 1998).

Based on the lithology, Dressler et al. (2003a) divided the sedimentary sequence of the impactite at Yax-1 into 6 units in descending order (Fig. 2). Unit 6 overlies the underlying limestone with irregular erosional surface, is 10.02 m thick (884.92–894.94 m), and is composed of a very coarse suevite with abundant carbonate and silicate melt fragments (Dressler et al. 2003a, b). Unit 5 overlies unit 6 with gradational contact (Dressler et al. 2003b), is 23.86 m thick (861.06–884.92 m), and is composed of coarse suevitic melt agglomerate with monomictly brecciated melt bodies (Dressler et al. 2003a, b). Unit 4 overlies unit 5 with sharp contact, is 15.26 m thick (845.80–861.06 m), and is composed of very coarse and heterogeneous melt agglomerate with fine-grained and homogeneous brownish matrix (Dressler et al. 2003a, b). Unit 3 overlies unit 4 with gradational contact, is 22.94 m thick (822.86–845.80 m), and is composed of coarse suevitic melt agglomerate with fine-grained and homogeneous brownish matrix (Dressler et al. 2003a, b). Unit 2 overlies unit 3 with irregular erosional surface, is 14.84 m thick (808.02–822.86 m), and is composed of pebble-sized suevite (Dressler et al. 2003a, b). The basal contact of the suevite in unit 1 was not observed due to the cracking of the core. However, the grain composition and size of unit 1 seems to change gradually from unit 2. Unit 1 is 13.39 m thick (794.63–808.02 m) and is composed of coarse sand to pebble-sized suevite (Dressler et al. 2003a). The suevite in units 1 and 2 is relatively well- sorted, and the grain size of the melt fragments and the carbonate lithics is small compared with those in units 3–6. The litho-stratigraphical division of Dressler et al. (2003a) is used in this study.

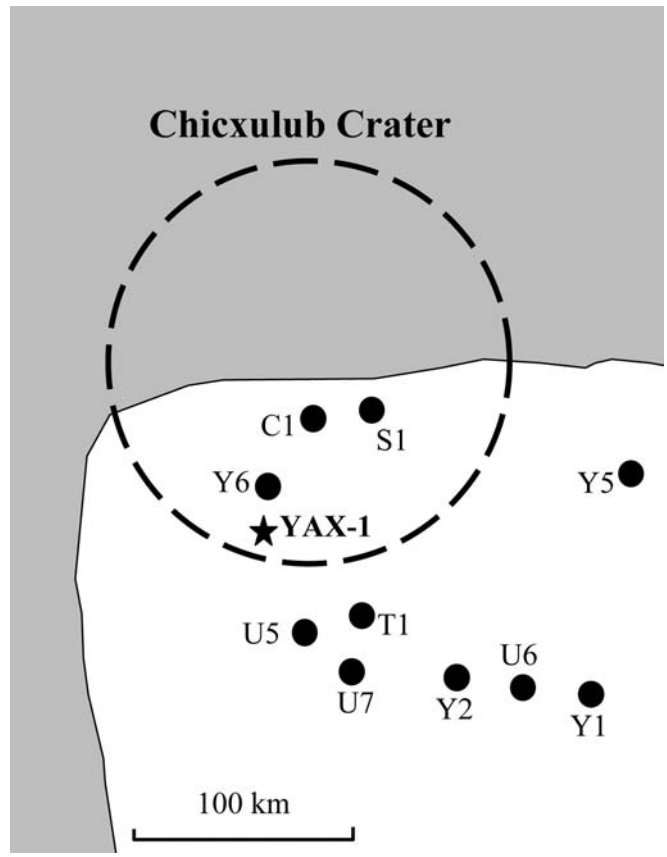

Fig. 1. A map showing locations of Yax-1 and other drilling sites in and around the Chicxulub crater (after Claeys et al. 2003).

Our own observations indicate that the lithology of an approximately 50 cm-thick interval of dolomitic calcarenite layer above unit 1 (794.14–794.63 m) is distinctly different from the underlying impactite and the overlying Tertiary sediments. However, no stratigraphic subdivision of this layer is proposed, and we refer to this layer as unit 0 (Fig. 2).

SAMPLES AND ANALYTICAL METHODS

Thirty-five samples were taken from unit 1 in Yax-1 at approximately 30 cm stratigraphic intervals between 795.58 and 807.27 m (Fig. 3) and subjected to detailed grain size and composition, chemical composition, and nannofossil biostratigraphic analyses. A similar number of samples was

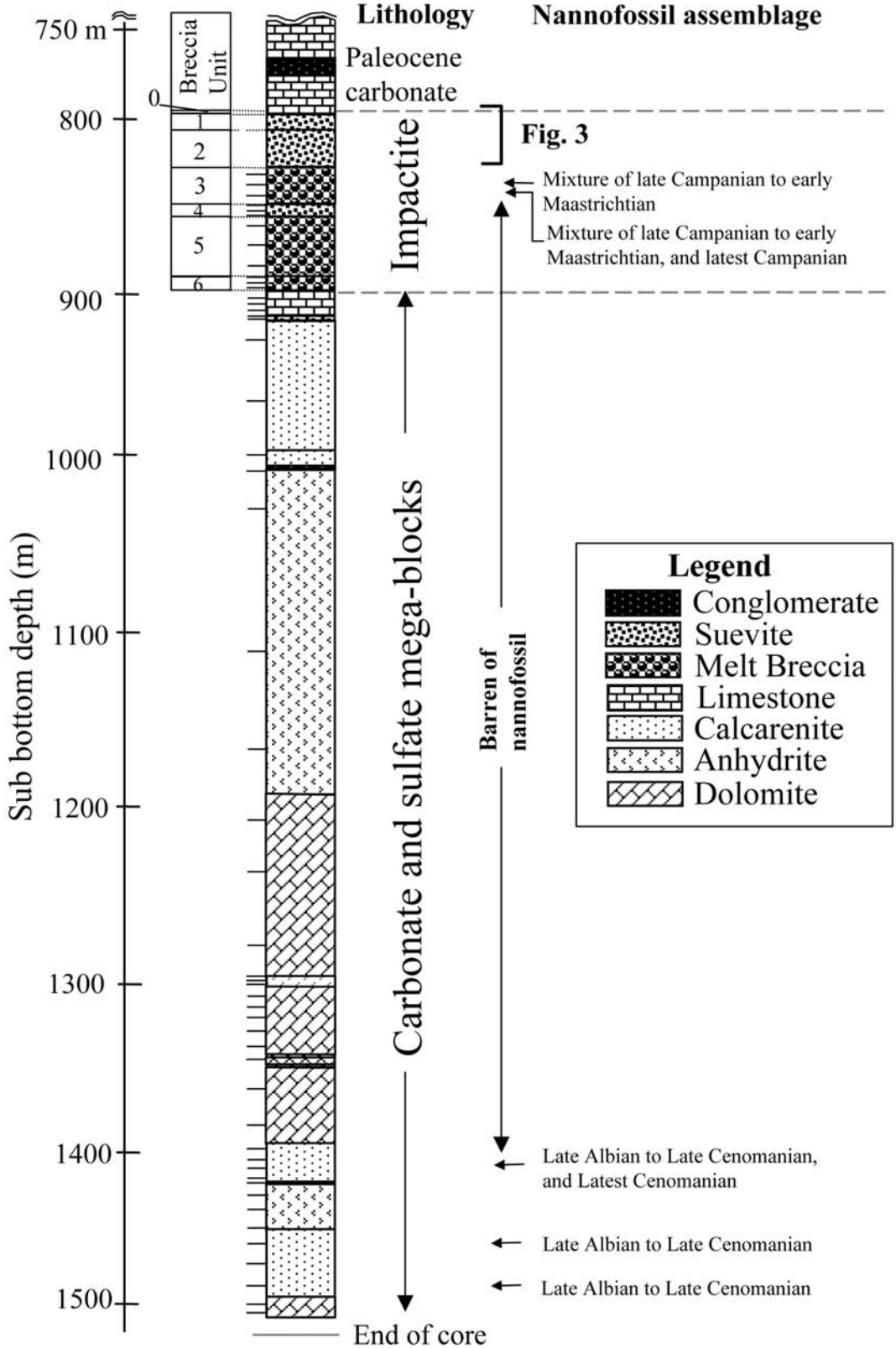

Fig. 2. A columnar section, its subdivision into units, and nannofossil assemblage of the Yax-1 core. Sampling horizons are also shown on the left side of the column (modified from lithological profile on CSDP Web site http://icdp.gfz-potsdam.de/html/sites/chicxulub/news/news.html). The litho-stratigraphical division is based on Dressler et al. (2003a).

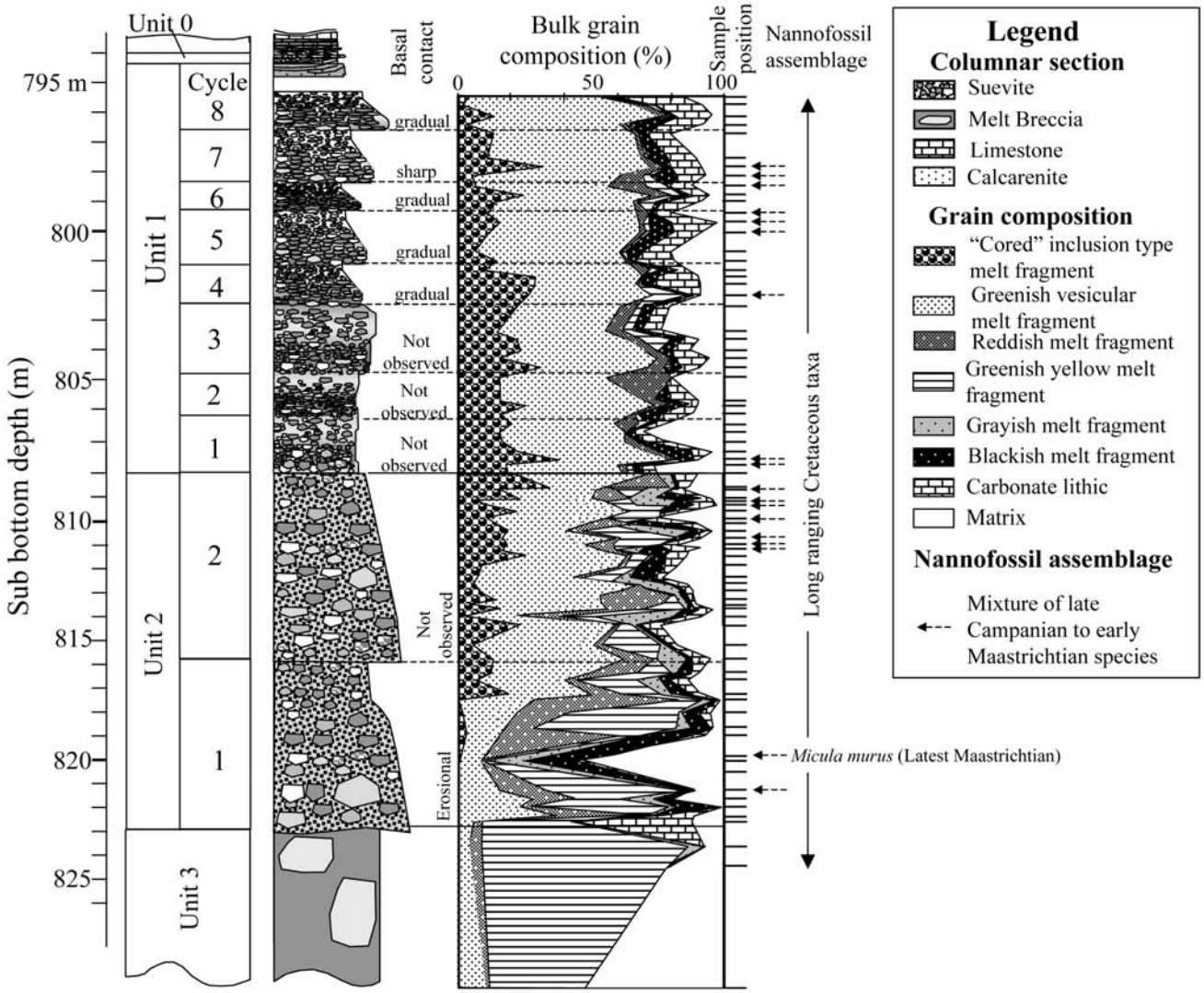

Fig. 3. A detailed columnar section, vertical variation of bulk grain composition, and nannofossil assemblage of units 2 and 1.

taken from the underlying carbonate and sulfate mega-blocks to determine their age using nannofossil biostratigraphy (Fig. 2). Forty samples were taken from unit 2, and 12 samples were taken from units 3–6 to compare grain composition with unit 1 and to investigate nannofossil biostratigraphy (Figs. 2 and 3). Three samples were taken from unit 0 to determine the exact position of the boundary between the impactite and the overlying Paleocene carbonate rock using nannofossil and planktonic foraminiferal biostratigraphy. All investigated samples were 10 cm^3 in volume.

Grain composition of 35 samples from unit 1 was investigated by point counting. We also investigated grain composition of 40 samples from unit 2 to compare it with that of unit 1. We investigated the components of the impactite and their textures, and composition of the matrix using thin sections. Furthermore, to investigate macroscopic variation of the grain composition, we took close-up digital pictures of rock surfaces in each sample and approximately 400 points were counted in these images. Suevite in units 2 and 1 are mainly composed of large (>2 mm) melt fragments and most of them are recognizable on rock surface based on their colors and textures.

Mineral composition of suevite samples was investigated by X-ray powder diffraction (XRD). Approximately 5 g of bulk sample was powdered in an agate mortar. The XRD analysis was conducted using a MAC Science MXP-3 X-ray powder diffractometer at the Department of Earth and Planetary Science, the University of Tokyo. The maximum sizes of carbonate grains and greenish silicate melt fragments in unit 1 were measured on each sample surface using micrometer calipers. Nannofossil assemblage was examined using an optical microscope. Planktonic foraminiferal assemblage was examined in thin sections.

Non-destructive, quantitative analyses of major element

composition and chemical mapping were conducted on polished sample surface using a Horiba XGT-2700 X-ray scanning microscope (XGT) at the Department of Earth and Planetary Science, the University of Tokyo. Analytical procedure is after Koshikawa et al. (2003). Bulk chemical composition of 5 major elements (Al, Si, Ca, Ti, and Fe) was measured on an approximately >1.5 cm^2 area for the 35 samples from unit 1 with XGT. We excluded the chemical composition data of Mg, K, and Mn due to the highly heterogeneous distribution of these elements.

RESULTS

Lithology and Petrography

We focused on the lithology and petrography of unit 1 to investigate the possibility of ocean water invasion into the crater. In this section, we describe lithology, grain composition, grain size, and chemical composition of unit 1 in detail. We further studied the lithology and petrography of units 2 and 0 to compare with those of unit 1.

Lithology and Petrography of Unit 2

Unit 2 overlies unit 3 with an irregular erosional contact (Fig. 4a). Unit 2 is approximately 15 m thick and is composed of highly heterogeneous suevite with abundant melt and lithic fragments. The suevite in unit 2 is poorly-sorted and shows clast-supported fabric (Fig. 4b). Unit 2 is basically composed of two normally-graded beds approximately 7 and 8 m thick (Fig. 3).

The suevite in each bed is composed of pebble- to cobble-sized, subangular to rounded, yellowish green, green, black, dark red, and brown silicate melt fragments with small amounts of limestone lithics and basement rock fragments. Large grayish melt fragments of up to 10 cm in diameter occur in the basal part of this unit. Content of yellowish green melt fragments is highly variable between 2 and 75 vol% of the suevite (Fig. 3). Most of the yellowish green melt fragments are larger than 1 cm.

Two types of greenish silicate melt fragments are recognized in this unit: the first type is greenish altered vesicular melt fragments, which are also observed in underlying unit 3 and are altered and replaced by smectite (Fig. 5a), and the other type are silicate melt-coated calcite grains (Fig. 5b). The latter type is similar to the "cored" inclusion type melt fragment that is interpreted as fallback ejecta (French 1998). The abundance of greenish altered vesicular melt fragments and "cored" inclusion type melt fragments is highly variable, between 6 to 52 vol% and 4–35 vol% of the bulk sample, respectively. Shocked quartz grains with planer deformation features (PDFs) are observed in unit 2. The PDFs are produced under pressure of 8–25 GPa (e.g., French 1998), suggesting that deposition of unit 2 was associated with the impact event. The matrix of the suevite in this unit is mainly composed of minute carbonate grains and coccoliths with small amount of minute melt fragments, quartz, and plagioclase grains.

Eight to ten small cyclic variations in grain composition are observed in upward fining beds of unit 2 (Fig. 3). These oscillations are characterized by the presence of extra large yellowish green melt fragments of more than 1 cm in diameter. Because unit 2 is highly heterogeneous and sizes of analytical samples are small (1 × 1 to 2 × 1.5 cm), it is difficult to justify the reliability of oscillations.

Lithology and Petrography of Unit 1

The basal contact of unit 1 was not observed due to the cracking of the core. However, the grain composition and size of unit 1 sediments seems to change gradually from unit 2. Unit 1 is approximately 13 m thick and is composed of relatively well-sorted suevite (Fig. 4c).

Unit 1 is composed of 1–2 m scale slight normally and/or inversely graded beds of suevite that repeated at least eight times (Fig. 3). These graded beds are named cycles 1–8 in ascending order. The basal contacts of cycles 1–3 have not been observed due to cracking of the cores at the boundaries. The basal contacts of cycles 4–8 are conformable. The basal contact between the cycles 6 and 7 is relatively sharp (Fig. 4d), while others are gradual. The suevite in each cycle shows repetition of clast-supported and matrix-supported fabrics. The maximum size of greenish vesicular melt fragments shows inverse plus normal grading in cycles 1–3, and normal grading in cycles 4–8 (Fig. 6a). On the other hand, the maximum size of limestone lithics shows normal grading in cycles 1–8 (Fig. 6a).

The major components of unit 1 are greenish vesicular melt fragments, "cored" inclusion type melt fragments, limestone lithics, and matrix. These 4 components comprise 80–90% of the suevite by volume (Fig. 3). Large yellowish green melt fragments, which are one of the major components of unit 2, are almost absent in unit 1. Limestone lithics occasionally contain small amount of planktonic foraminifera (Fig. 5c). The matrix is mainly composed of minute carbonate grains, coccoliths, calcite grains, small amount of minute melt fragments, quartz, and plagioclase grains. The abundance of greenish vesicular melt fragments and limestone lithics increases upward, while the abundance of "cored" inclusion type melt fragments and calcareous matrix decreases (Fig. 3). Oscillations in grain composition correspond to the individual cycles and are characterized by variation in the relative abundance of fragments of limestone lithics, silicate melt fragments, and calcareous matrix (Fig. 3). Shocked quartz grains with PDFs (Fig. 5d) are observed throughout unit 1, suggesting that deposition of unit 1 was associated with an impact event.

Table 1 shows the bulk chemical compositions of Al, Si,

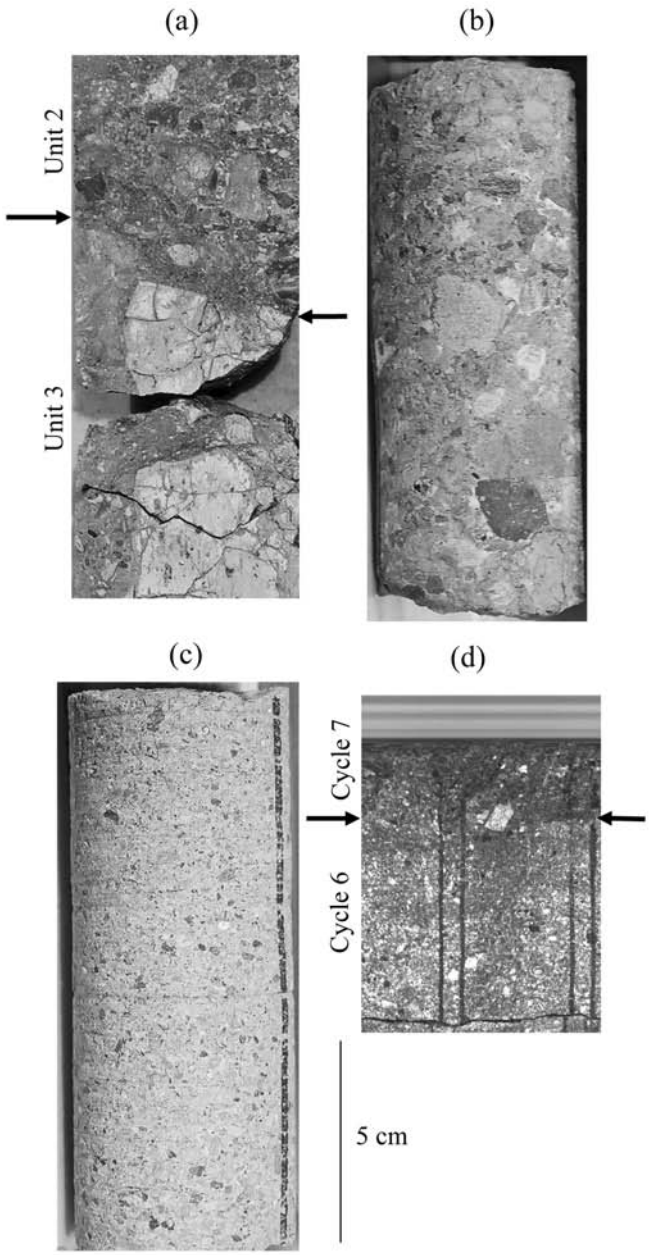

Fig. 4. Core photographs of: a) an irregular erosional contact between units 3 and 2 (arrows); b) the poorly-sorted suevite in unit 2 (817.78–817.93 m); c) the well-sorted suevite in unit 1 (799.21–799.36 m); and d) a conformable and sharp contact between cycles 6 and 7 of unit 1. Photo (d) is a photo of a piece taken by UNAM using an unrolled core scan (360°).

Ca, Ti, and Fe in the suevite of unit 1. Oscillations in the bulk chemical compositions are also recognized in association with cycles 1–8 (Fig. 6b) and are regarded as representing a variation in the ratio of the two components; one is characterized by higher content of Ca and the other is characterized by higher contents of Si, Fe, Ti, and Al (Fig. 6b). Calcium is concentrated in the calcareous matrix, although a small amount is held in the limestone lithics, while Si, Fe, Ti, and Al are concentrated in the silicate melt fragments. As a result, higher Ca content implies larger matrix content. This is consistent with the observation that higher Ca samples in the upper part of each cycle show matrix supported fabric (Figs. 7a and b), while lower Ca samples in the lower part of each cycle show clast-supported fabric (Figs. 7c and d).

Approximately 20 cm interval of the uppermost part of unit 1 (794.63–794.79 m) is composed of greenish, medium to coarse-grained sandstone with parallel to mono-directional cross lamination (Fig. 8), suggesting that an ocean current influenced the deposition of this interval.

Lithology and Petrography of Unit 0

Unit 0 is approximately 50 cm thick, conformably overlies unit 1 (Fig. 8), and is mainly composed of light gray dolomitic very fine calcarenite. The dolomitic calcarenite is interbeded with seven ~2 cm-thick greenish suevitic beds (Fig. 8). Dolomitic calcarenite is mainly composed of light gray dolomite grains and micrite. Rhombohedral dolomite grains in unit 0 are of probable authigenic origin. Cross laminations, which are unidirectional current cross-lamina with climbing structure (Fig. 8), are observed in the lower 20 cm of this unit, while faint parallel lamination is observed in dolomitic calcarenite in the middle 20 cm of this unit (Fig. 8). A 2 cm-thick black clay layer overlies this unit with probable parallel unconformity (Fig. 8; 794.12–794.14 m).

Age Constraints of Carbonate Mega-Blocks, Impactite, and Unit 0 in the Yax-1 Core

Sediments underlying the impactite (>894.94 m) are composed of probable mega-blocks of calcarenites, limestones, dolostones, and anhydrites which were probably formed as a result of collapse of the rim caused by the impact (Kenkmann et al. 2003; Wittmann et al. 2003). Nannofossil assemblages of two calcarenite samples from 1474.49 m and 1457.51 m in the lower part of carbonate mega-blocks contain *Lithraphidites acutum, Axopodorhabdus albianus, Microstaurus chiastius, Eprolithus floralis,* and *Rhagodiscus asper* suggesting a late Albian to late Cenomanian age. Furthermore, nannofossil assemblages of a calcarenite sample from 1407.44 m also contains *Microstaurus chiastius,* which is older than the latest Cenomanian. Consequently, the age of lower part of carbonate and sulfate mega-blocks are older than the latest Cenomanian (Fig. 2). The middle to upper part of carbonate and sulfate mega-blocks is almost barren of nannofossils, so their ages are uncertain (Fig. 2).

Units 6 to 4 are almost barren of nannofossils. Samples from 823.24 and 823.56 m in unit 3 contain a mixture of species which combined suggest a late Campanian to early Maastrichtian age (Fig. 2; *Quadrum trifidum, Quadrum gothicum,* and *Eiffellithus eximius*). The sample from

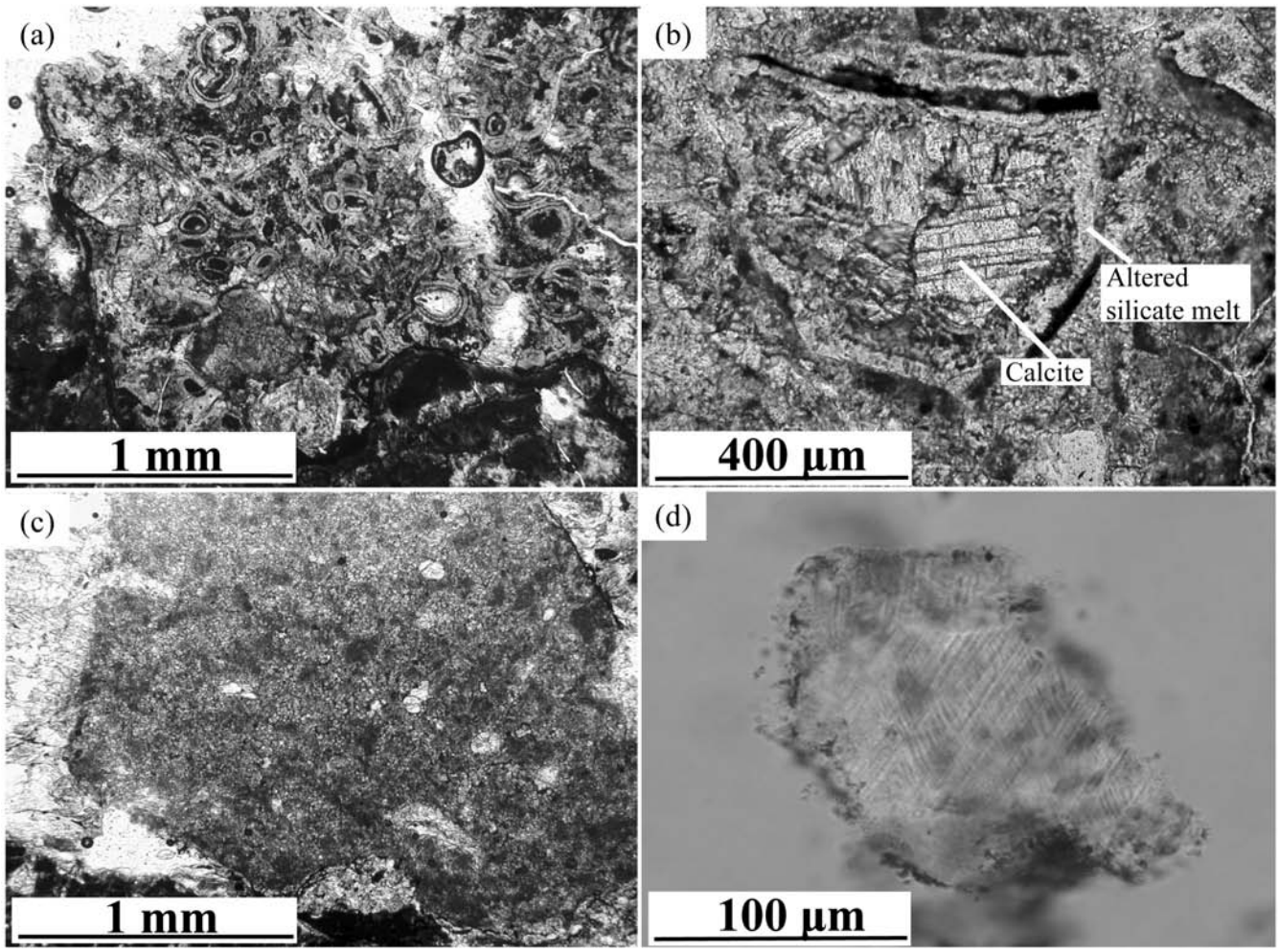

Fig. 5. Thin section photomicrographs of: a) greenish altered vesicular melt fragments in unit 3 (840.7 m, open nicol), and b) a "cored" inclusion type melt fragment, which is composed of silicate melt-coated calcite grains and is interpreted as fall back ejecta, in unit 2 (810.23 m, open nicol); c) a limestone lithic in unit 2 (810.23 m, open nicol); and d) a shocked quartz grain with three sets of PDFs in unit 1 (794.90 m, open nicol).

823.56 m also contains one specimen of *M. chiastius* (Fig. 2). *M. chiastius* in unit 3 may have been derived from underlying carbonate mega-blocks because *M. chiastius* is also found in the lower part of carbonate mega-blocks. On the other hand, there is no late Campanian to early Maastrichtian nannofossils in carbonate mega-blocks, suggesting that nannofossils of late Campanian to early Maastrichtian age was derived not from underlying carbonate mega-blocks but from outside the crater.

Nannofossil assemblages of units 2 and 1 are the mixture of diagnostic species the co-occurrence of which suggests a range from late Campanian to early Maastrichtian (*Quadrum trifidum, Eiffellithus eximius, Tranolithus orionatus, Aspidolithus parcus,* and *Quadrum gartneri*). Samples also contain numerous long-ranging Cretaceous taxa (Fig. 3). Even though there could be numerous source horizons for these reworked nannofossils (as discussed in Bralower et al. (1998) for the "cocktail" assemblages in the Gulf of Mexico), we interpret the minimum source of late Campanian to early Maastrichtian for the diagnostic species. One specimen of *Micula murus,* which is the latest Maastrichtian in age, is found in a sample from the basal part of unit 2 (Fig. 3; 819.96 m). Mixed nature of reworked microfossils including latest Maastrichtian age, lithic fragments, and impact derived materials in the suevite of units 2 and 1 is similar to the K/T boundary "cocktail" deposits in the Gulf of Mexico (Bralower et al. 1998), suggesting that units 2 and 1 in Yax-1 core were related to the K/T boundary impact and were formed as a result of reworking.

Unit 0 is barren of nannofossils and planktonic foraminifera (Fig. 8). The lowermost Danian (P0) is absent based on planktonic foraminifera (Smit et al. 2003), and Ir anomaly data has not been reported. Therefore, the boundary between the impactite and Paleocene may be an unconformity, although we cannot still exclude the possibility that the boundary is within unit 0.

Table 1. Bulk chemical composition of the suevite in unit 1 (wt%) determined by XGT.

Sample number	Cycle	Sub-bottom depth (m)	Al_2O_3 (wt%)	SiO_2 (wt%)	CaO (wt%)	TiO_2 (wt%)	Fe_2O_3 (wt%)
1277	8	795.58	10.18	37.33	18.54	0.44	4.59
1278	8	795.87	12.26	44.54	9.49	0.54	5.64
1279	8	796.18	12.83	46.81	10.71	0.53	5.58
1280	8	796.47	11.06	40.67	9.32	0.51	5.16
1281	7	796.76	10.61	39.03	20.50	0.46	4.39
1126	7	797.52	11.45	40.19	11.15	0.50	5.18
1127	7	797.83	11.82	49.36	6.83	0.61	6.17
1128	7	798.15	12.96	49.46	7.61	0.59	5.78
1129	6	798.45	11.13	40.89	15.50	0.49	4.96
1130	6	798.74	11.69	45.40	8.59	0.56	5.62
1131	6	798.96	10.79	43.58	10.22	0.53	5.75
1133	5	799.32	11.72	40.47	16.57	0.46	4.92
1134	5	799.62	11.38	43.56	10.79	0.52	5.33
1135	5	799.92	11.72	49.00	7.36	0.56	6.00
1137	5	800.55	12.09	44.20	6.77	0.53	5.69
1138	5	800.85	11.62	41.63	10.81	0.51	5.23
1139	4	801.15	9.41	33.68	20.29	0.41	4.23
1140	4	801.34	12.12	46.39	8.17	0.53	5.54
1141	4	801.61	12.49	47.15	6.66	0.58	5.94
1142	4	801.96	12.71	47.98	6.78	0.57	5.88
1143	3	802.31	10.82	35.19	22.17	0.45	4.03
1145	3	803.08	10.72	38.71	17.79	0.52	4.40
1146	3	803.38	13.16	44.46	11.98	0.55	5.09
1147	3	803.68	11.21	43.08	13.54	0.51	5.21
1148	3	803.98	10.98	45.21	8.70	0.56	5.67
1149	3	804.28	12.92	49.19	7.82	0.59	5.87
1150	2	804.58	10.55	37.04	19.21	0.46	4.87
1151	2	805.28	11.76	43.91	11.70	0.52	5.48
1152	2	805.47	12.21	46.41	7.87	0.56	6.10
1153	2	805.77	11.38	44.56	8.97	0.52	5.50
1154	1	806.07	10.70	38.03	21.26	0.47	4.59
1155	1	806.37	10.49	38.89	16.92	0.45	4.49
1156	1	806.67	10.37	37.68	15.16	0.47	4.50
1157	1	806.97	12.22	46.09	8.54	0.54	5.68
1158	1	807.27	12.35	47.11	8.42	0.57	5.91

The first appearance of Danian planktonic foraminifera (*P. eugubina*) is just above the black clay layer (Fig. 8, according to Keller et al. 2003). Smit et al. (2003) reported that Paleocene fauna corresponding to *G. eugubina* zone appears 5 cm above the black clay layer (Fig. 8; 794.07 m). The sample from 793.94 m contains abundant biserial heterohelicids and globigerine specimens larger than 0.3 mm in size, and a single specimen of *Globigerinelloides*-like planispiral genus. These planktonic foraminifers suggest Cretaceous age and are possibly reworked. Very thin-walled individuals are preserved among thick-walled specimens, indicating that dissolution has not substantially modified the depositional assemblage. The sample from 793.94 m also contains nannofossils *Thoracosphaera* and *Braarudosphaera* that occur right after the impact. In addition, very small specimens of *Cruciplacolithus primus* are also observed in this sample (Fig. 8), suggesting an age younger than 64.8 Ma (C29r, P1a) according to Berggren et al. (1995).

DISCUSSION

The Possibility of Ocean Water Invasion and Sedimentary Process of Units 2 to 1

Mixed nature of reworked microfossils including latest Maastrichtian age, lithic fragments, and impact derived materials such as shocked quartz grains with PDFs in the suevite of units 2 and 1 is similar to the K/T boundary "cocktail" deposits in the Gulf of Mexico (Bralower et al. 1998), suggesting that units 2 and 1 in Yax-1 core were related to the K/T boundary impact and were formed as a result of reworking.

Although the K/T boundary sequence in Yax-1 core may not be stratigraphically complete, sedimentological data provide compelling evidence for events immediately after the impact. Reworked nannofossils of late Campanian to early Maastrichtian age are abundant in the matrix of units 2 and 1.

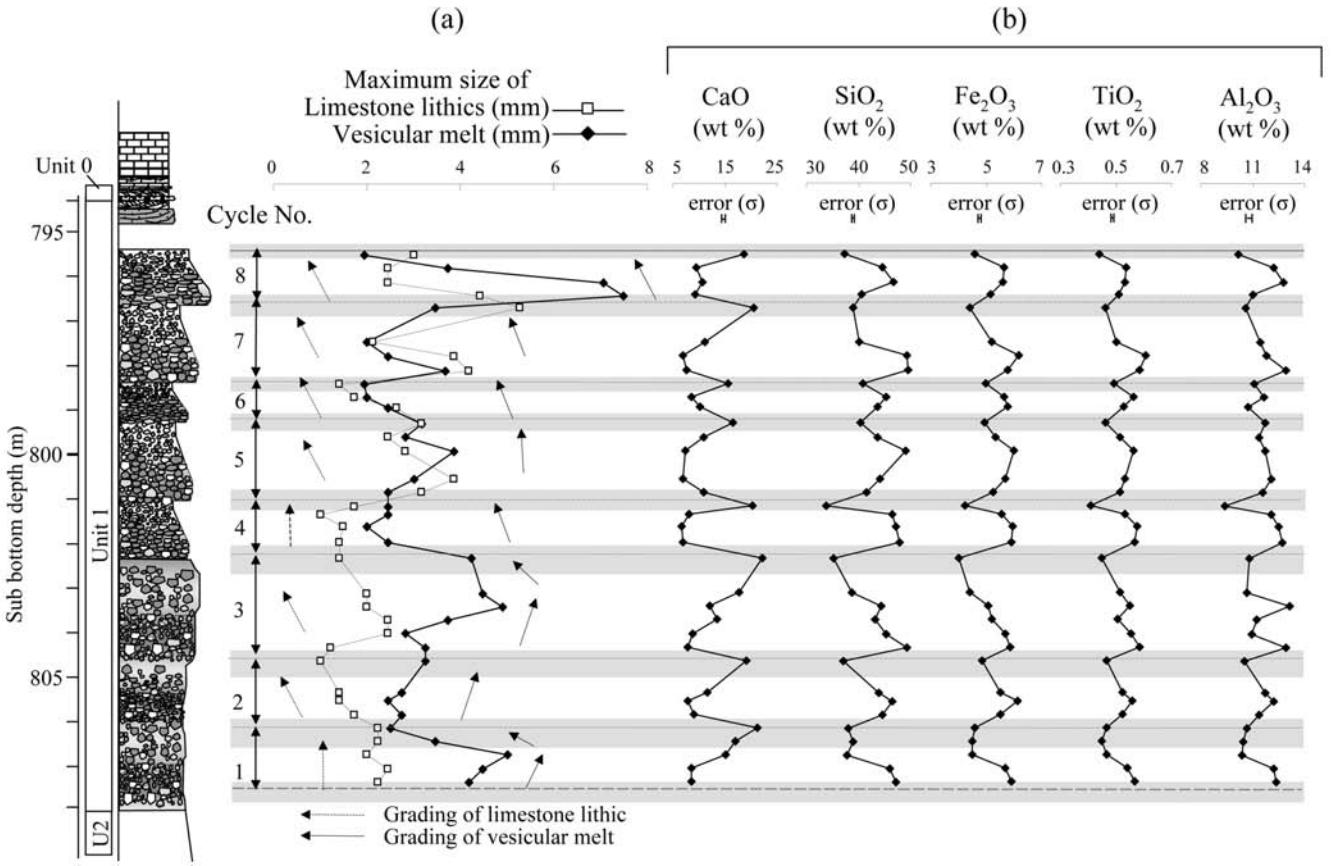

Fig. 6. a) A diagram showing vertical variations of maximum size of limestone lithics (mm) and greenish vesicular melt fragments. The arrows of dashed and solid lines indicate normal or inverse grading of limestone lithics and greenish melt fragments in each cycle, respectively. The shades indicate intervals of high calcium content in each cycle; b) diagrams showing vertical variations of chemical composition of the suevite in unit 1 (wt%) determined by XGT.

It is important to note that this age range is considerably narrower than the range of the sediments excavated by the crater formation. This suggests that these nannofossils were selectively incorporated in units 2 and 1. There is no late Campanian to early Maastrichtian nannofossils in carbonate mega-blocks underneath the impactite in Yax-1, suggesting that these nannofossils were not derived from underlying carbonate mega-blocks. These nannofossils (also the limestone lithics) cannot have been derived from the ejecta plume because they show no signs of recrystallization or melting. Therefore, nannofossils (also the limestone lithics) in units 1 and 2 were probably derived from unconsolidated carbonate sediments deposited outside the crater, within the ejecta curtain deposits, or from the rim wall.

Study of the Tvären crater in Sweden, which is 2 km in diameter and was formed on the floor of an ocean 100–150 m deep (Ormö and Lindström 2000), has documented resurge deposits in the upper part of the impactite formed by the ocean water invasion immediately after the impact (e.g., Ormö and Lindström 2000). These resurge deposits tend to show the reversed chronology (Ormö and Lindström 2000). Namely, the lower part of the deposit consists of the particles derived from younger sediments and the upper part consists of the particles derived from older sediments (Ormö 1994; Ormö and Lindström 2000). This is because ocean floor sediments outside the crater were eroded by currents and transported into the crater beginning with younger units and progressing to older units (Ormö and Lindström 2000). In the case of the suevite in Yax-1 core, nannofossil assemblage of the major part of units 1 and 2 are of late Campanian to early Maastrichtian age, while the only latest Maastrichtian nannofossil is observed in the basal part of unit 2. Thus, the most probable mechanism of erosion and transportation of the nannofossils in the unconsolidated carbonate sediments of the inner rim margin and/or outside the crater is via ocean water invasion.

If carbonate sediments of Campanian to Maastrichtian age outside the crater were eroded by the surge of ocean water into the crater, the sedimentary sequence outside the crater should have a hiatus corresponding to this age range. Alternatively, collapse of the rim wall and ejecta curtain deposits on the rim by the ocean water invasion or the impact seismic wave also could have supplied sediment particles with nannofossils of Campanian to Maastrichtian age into the

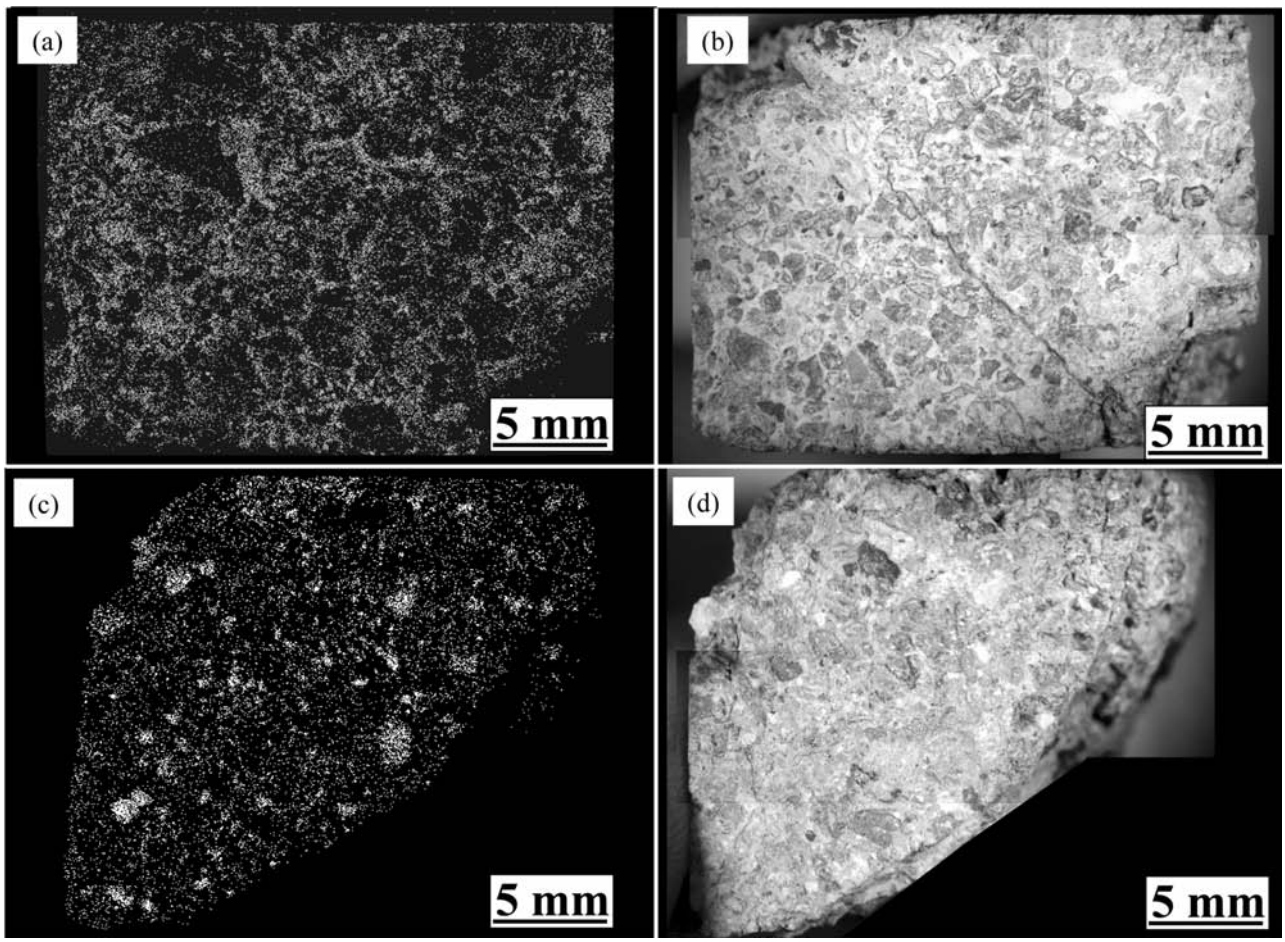

Fig. 7. a) A calcium distribution map and b) a rock surface photograph of higher calcium content sample from 802.31 m in unit 1. Higher calcium sample shows matrix-supported fabric; c) a calcium distribution map, and d) a rock surface photograph of lower calcium content sample from 801.96 m of unit 1. The lower calcium sample shows clast-supported fabric.

crater. In this case, the age range of nannofossils in the crater rim and ejecta curtain deposits outside the rim should be dominated by Campanian to Maastrichtian age. However, no information is available on the age of the impactite outside the crater. Further detailed research of the impactite outside the crater is needed to determine the source of carbonate sediments of Campanian to Maastrichtian age in units 2 and 1.

Unit 2 is composed of two normally graded beds (Fig. 3). Irregular erosional basal contact, poor sorting, clast-supported fabric, and the occurrence of intraclast-like melt fragments at the base of the lower bed suggest that this unit was deposited by gravity flows (e.g., Middleton and Hampton 1976). The presence of nannofossils, probably derived from outside the crater, indicates that gravity flows were formed in association with ocean water invasion. Alternatively, if the collapse of the rim wall and ejecta curtain deposits accumulated on the rim were the sources of nannofossils, impact seismic wave may have triggered gravity flows. In this case, gravity flows may have run down on the rim surface in association with the ocean water invasion or under the hot/dry conditions without influence of water invasion.

The suevite in unit 1 is well-sorted and shows upward fining of limestone lithics in each cycle. This indicates that the suevite in each cycle in unit 1 was deposited as a result of settlement of re-suspended sediment particles. Furthermore, there is no erosional surface at the base of each cycle, suggesting that coarse sediment particles, which probably were derived from outside the crater and/or crater rim, probably have been transported in suspension by water mass movement. Therefore, repeated ocean water invasion is the most probable mechanism for the cyclic sedimentation of the suevite in unit 1. Repeated forceful ocean water invasion is probably required to transport mm-size grains in each cycle as suspension.

Similar cycles are also reported from the impactite in the Chesapeake Bay crater (Poag et al. 2002). The Chesapeake Bay crater is 85 km in diameter and is buried 300–500 m below the floor of the southern part of the Chesapeake Bay (Poag et al. 1994, 2002). Poag et al. (2002) mentioned that the upper part of the impactite in the Chesapeake Bay crater consists of repeating upward fining beds. They interpreted these cycles to have been formed by repeated ocean water

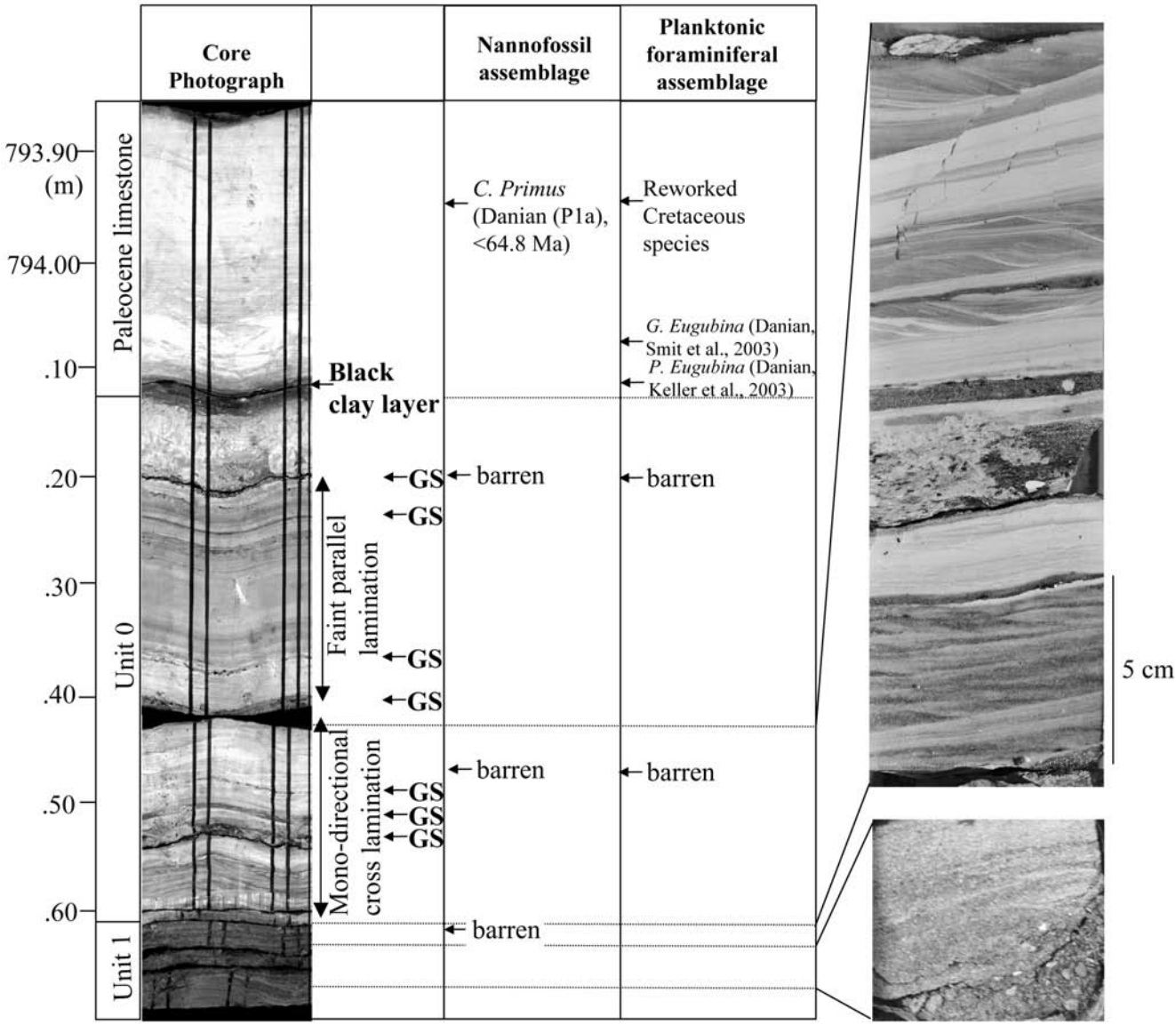

Fig. 8. A core photograph of the uppermost part of unit 1, unit 0, and the overlying Paleocene carbonate (793.97–794.63 m). Nannofossil and planktonic foraminiferal assemblage are also shown. The left-side photo is a photo of a piece taken by UNAM using an unrolled core scan (360°). The right-side photos show half cut surfaces of the uppermost part of unit 1 and the basal part of unit 0. Parallel and mono-directional cross laminations are observed in these intervals. GS = greenish suevitic bed.

invasion based on facies analysis of cores and downhole geophysical logs. Similarity in cyclic sedimentation pattern in the upper part of the impactite both in the Chicxulub crater and the Chesapeake Bay crater supports our interpretation that unit 1 in Yax-1 was probably formed by lateral supply of coarse sediments through repeated ocean water invasion into the crater cavity.

The thicknesses of cycles are 7–8 m in unit 2 and 1–2 m in unit 1 at Yax-1. These thicknesses seem thin for repeated forceful ocean water invasion (= resurge) when compared with the thicknesses of the resurge deposits in other marine target craters. However, this could be owing to the position of Yax-1, which is located near the edge of the crater rim and well above the crater floor. In fact, the suevite reaches the thickness of ~300 m at C1, S1, and Y6 cores (Sharpton et al. 1996; Claeys et al. 2003) that are located in the central part of the crater (Fig. 1).

The presence of parallel and mono-directional cross laminations in the uppermost part of unit 1 and the lower part of unit 0 suggests that the crater was already filled with water and that sedimentation of this interval was under the influence of currents. Cross lamination is one of the typical characters of the resurge deposits and is also found in other marine target impact craters such as the Lockne crater in Sweden (Dalwigk and Ormö 2001), which is ~13.5 km in diameter and was formed on the ocean floor in water over 200 m deep (Ormö

and Lindström 2000). According to Ormö and Lindström (2000), the lower part of the resurge deposits in the resurge gullies of the Lockne crater is matrix-supported and is similar to debris flow deposit. The upper part is clast-supported and has a relatively high proportion of crystalline ejecta clasts (Ormö and Lindström 2000). The uppermost fine-grained part of the resurge deposit displays current lineation, cross-bedding, and dewatering structures (Dalwigk and Ormö 2001). Upward fining character of the impactite and the presence of cross-bedding in the uppermost part of the resurge deposits of the Lockne crater is similar to those of units 2 to 0 in Yax-1, implying that units 2 to 0 in Yax-1 were probably formed by ocean water invasion similar to the resurge deposits in the Lockne crater.

Cross-lamination represents a lower energy flow regime (e.g., Middleton and Southard 1977), but its occurrence in the uppermost part of the impactite could suggest deposition during the waning stages of current flow. Similar cross-lamination is reported from the top of the impactite in UNAM 5 (U5) core (Smit 1999), which is located approximately 110 km to the south of the center of the Chicxulub crater, probably on the outside slope of the crater (Fig. 1). This suggests that the influence of currents was not local but prevailed both inside and outside the crater.

The Timing of Ocean Water Invasion

The maximum size of limestone lithics in unit 1 shows a number of repeated depositional units with normal grading, while the maximum size of greenish vesicular melt fragments shows inverse plus normal grading in cycles 1–3 and normal grading in cycles 4–8 (Fig. 6a).

Large, intact porous fragments such as pumice commonly have low bulk density and are likely deposited slowly through the atmosphere and water column, while small pumice probably sink rapidly because most bubble walls are broken or cracked (e.g., Fisher and Schmincke 1984). Inverse grading of pumice fragments results from the time lag between the deposition of the large and lower density, and small and higher density, pumice fragments (e.g., Fisher and Schmincke 1984). Therefore, formation of inverse grading of greenish vesicular melt fragments in cycles 1–3 can be explained by a lag of sedimentation between the larger and smaller melt fragments due to the differences in their bulk densities. On the other hand, normal grading of greenish vesicular melt fragments in cycles 4–8 likely occurred after water infiltrated into the pores and increased their bulk densities.

Infiltration of water into vesicular grains typically occurs within minutes to hours of their contact with water, although infiltration time of water is dependent on the chemical composition and the size of the grain (e.g., Fisher and Schmincke 1984). Greenish vesicular melt fragments observed in units 2 and 1 is <8 mm. If we assume that the greenish vesicular melt fragments were ejected to the upper layer of the atmosphere by the impact and then settled through the atmosphere and the ocean water, the greenish vesicular melt fragments probably reached the ocean surface within an hour of the impact. Therefore, sedimentation of cycles 1–3 may have started within several hours after the impact.

Partial or complete collapse of the crater rim is required for ocean water to enter the crater cavity immediately after the impact. The water depth of the impact site is estimated as less than 100 m at the time of the impact (Sharpton et al. 1996; Pierazzo and Crawford 1997; Pierazzo et al. 1998). On the other hand, the transient crater rim was estimated to be several km in height at the K/T boundary impact (e.g., Morgan et al. 2000). Consequently, if the transient crater rim had not collapsed immediately after the impact, it should have prevented ocean water from invasion into the crater.

However, the transient crater rim is normally very unstable, especially in the case of large crater such as the Chicxulub crater, and thus, likely collapsed immediately after the crater formation (e.g., Morgan et al. 1997, 2000; Collins et al. 2002). Cretaceous mega-blocks (evidence for rim collapse) are reported in Yax-1 (Kenkmann et al. 2003; Wittmann et al. 2003). Furthermore, a vertical offset of at least 2 km is indicative of the collapse of the crater rim, and a high elevation of the crater rim was not observed in the seismic reflection data (e.g., Morgan et al. 1997). According to numerical simulations, the transient crater rim could have been temporarily elevated several km from the pre-impact surface, but it could have collapsed into the crater within minutes after the impact (Morgan et al. 2000; Collins et al. 2002). Furthermore, the final crater shape of their numerical simulation is similar to the crater shape of the Chicxulub crater, and a high elevation of the final crater rim was not observed (Morgan et al. 2000; Collins et al. 2002).

In this way, drilling core data, seismic reflection data, and numerical simulation data suggest that the rim of the Chicxulub crater may have partially or entirely collapsed immediately after the impact. Therefore, ocean water could have surged into the Chicxulub crater immediately after the impact in spite of the shallow water depth of the site before the impact.

Implication for the Tsunami Generation Mechanism

Two different generation mechanisms have been proposed for the giant tsunami of the K/T boundary (e.g., Matsui et al. 2002): one is a tsunami generated by landslides on the slope of the Yucatán Platform triggered by the shock wave from the impact point (hereafter, we call it landslide-generated tsunami) and the other is a tsunami generated by ocean water invasion into the crater and subsequent overflow of water (hereafter, we call it crater-generated tsunami).

Large-scale erosion of the Cretaceous sediments caused by the K/T boundary impact (Bralower et al. 1998; Tada et al. 2002) and over 250 m-thick K/T boundary deposits of

probable gravity flow origin have been documented on the continental slope around the Yucatán Peninsula (Grajales-Nishimura et al. 2000; Kiyokawa et al. 2002). These large-scale gravity flows could have caused landslide-generated tsunami, which in turn could have affected the sedimentation of the K/T boundary deposits around the proximal impact site (Bralower et al. 1998; Kiyokawa et al. 2002; Matsui et al. 2002).

On the other hand, the results of this study also suggest that ocean water invasion into the crater probably occurred immediately after the impact. Cyclic sedimentation of unit 1 implies repeated water mass movements within the crater that were forceful enough to carry mm-size grains as suspension. Such forceful water mass movements could have been caused by repeated ocean water invasion and may have caused crater-generated tsunami. Therefore, the crater-generated tsunami possibly could have also been another generation mechanism of tsunami at the K/T boundary. Numerical simulation of the K/T boundary tsunami by Matsui et al. (2002) suggests that the wave height of crater-generated tsunami could have been several tens of meters around the coastal area of the Gulf of Mexico, even if the water depth of the Yucatán platform were very shallow. The tsunami of this magnitude has enough power to cause suspension of sandy particles on the ocean bottom (e.g., Kastens and Cita 1981; Bryant 2001). Therefore, crater-generated tsunami may also have affected the sedimentation of the K/T boundary deposits.

However, we need more information to evaluate the influence of ocean water invasion into the Chicxulub crater on the ocean environment outside the crater. The results presented here are based on the observations at a single but the only available core. Furthermore, number, direction, and magnitude of crater-generated tsunami is dependent on various parameters such as the target water depth and the scale and range of the crater rim collapse (Matsui et al. 2002). Therefore, further core drilling inside and outside the crater for comparison with the results of Yax-1 and numerical calculations based on stronger geological constraints are required to discuss the number, direction, and magnitude of crater-generated tsunami and their influence on the sedimentation of the K/T boundary deposits. The drilling into the Chicxulub crater planned by the Integrated Ocean Drilling Program (IODP) will enable us to discuss the role of ocean water invasion into the crater just after the K/T boundary impact.

SUMMARY

Lithology, grain composition, chemical composition, grain size, and nannofossil assemblage were examined in the Yax-1 core to investigate the possibility of the ocean water invasion into the Chicxulub crater immediately after the impact. An impactite occurs within the interval between approximately 794.63 and 894.94 m depth and is divided into 6 units in descending order. In this study, we mainly focused on the sedimentary process of units 1 and 2 because this part is deposited in the uppermost part of the impactite and probably was deposited during the latest stage of the formation of the Chicxulub crater.

Unit 2 is composed of highly heterogeneous suevite with abundant melt and lithic fragments and contains two normally graded beds. On the other hand, unit 1 is composed of relatively well-sorted suevite and contains at least eight 1–2 m-scale normally and/or inversely graded beds of the suevite.

Abundant nannofossils of late Campanian to early Maastrichtian age in the matrix of units 2 and 1 suggests that carbonate sediments deposited in the inner rim margin or around the crater were selectively eroded and transported into the crater, most likely by ocean water invasion into the crater. The occurrence of parallel and mono-directional cross lamination in the uppermost part of unit 1 and the lower part of unit 0 suggests the influence of current at least during the deposition of this interval. Given the infiltration time of water into the greenish vesicular melt fragments in unit 1, ocean water invasion probably started immediately after the impact. This is supported by the presence of vertical offset and the absence of a high crater rim, suggesting the collapse of the crater rim immediately after the impact.

Irregular erosional basal contact, normal grading, poor sorting, clast-supported fabric, and the occurrence of intraclast-like melt fragments at the base of the suevite in unit 2 suggest that this sub-unit was formed by gravity flows that were probably triggered by ocean water invasion or an impact seismic wave. On the other hand, the upward fining grain size and the absence of erosional contact of each cycle in unit 1 probably indicate that each cycle has been deposited from re-suspended sediment particles transported as suspension by water mass-movement in association with ocean water invasion.

Acknowledgments–This research is based on samples and data provided by the Chicxulub Scientific Drilling Program (CSDP) sponsored by International Continental Scientific Drilling Program (ICDP) and Universidad Nacional Autónoma de México (UNAM). We wish to thank J. U. Fucugauchi, J. Smit, and A. M. Soler Arechalde, for their support during sampling. We also wish to thank staffs of the Japanese ICDP office for their support during submission of our proposals. We also thank P. Claeys, H. Dypvik, J. Ormö, D. King, F. Imamura, and F. Masuda for their critical reading of the manuscript and for many valuable suggestions. This research was partly funded by the Japanese Society for the Promotion of Science (JSPS) Fellowship provided to K. Goto.

Editorial Handling—Dr. Philippe Claeys

REFERENCES

Berggren W. A., Kent D. V., Swisher C. C., and Aubry M. P. 1995. A revised Cenozoic geochronology and chronostratigraphy. In

Geochronology, time scales, and global stratigraphic correlation, edited by Berggren W. A., Kent D. V., Aubry M. P., and Hardenbol J. Special Publication 54. Society of Economic Paleontologists and Mineralogists. pp. 129–212.

Bourgeois J., Hansen T. A., Wiberg P. L., and Kauffman E. G. 1988. A tsunami deposit at the Cretaceous-Tertiary boundary in Texas. *Science* 241:567–570.

Bralower T. J., Paul C. K., and Leckie R. M. 1998. The Cretaceous/Tertiary boundary cocktail: Chicxulub impact triggers margin collapse and extensive sediment gravity flows. *Geology* 26: 331–334.

Bryant E. 2001. Tsunami: The underrated hazard. Cambridge: Cambridge University Press. 320 p.

Claeys P., Heuschkel S., Lounejeva-Baturina E., Sanchez-Rubio G., and Stöffler D. 2003. The suevite of drill hole Yucatán 6 in the Chicxulub impact crater. *Meteoritics & Planetary Science* 38: 1299–1317.

Collins G. S., Melosh H. J., Morgan J. V., and Warner M. R. 2002. Hydrocode simulations of Chicxulub crater collapse and peak-ring formation. *Icarus* 157:24–33.

Dalwigk I. and Ormö J. 2001. Formation of resurge gullies at impacts at sea: The Lockne crater, Sweden. *Meteoritics & Planetary Science* 36:359–369.

Dressler B. O., Sharpton V. L., Morgan J., Buffler R., Moran D., Smit J., Stöffler D., and Urrutia J. 2003a. Investigating a 65 Ma-old smoking gun: Deep drilling of the Chicxulub impact structure. *EOS Transactions* 84:130.

Dressler B. O., Sharpton V. L., and Marin L. E. 2003b. Chicxulub Yax-1 impact breccias: Whence they come? (abstract #1259). 34th Lunar and Planetary Science Conference. CD-ROM.

Fisher R. V. and Schmincke H. U. 1984. *Pyroclastic rocks.* Berlin-Heidelberg: Springer-Verlag. 472 p.

French B. M. 1998. *Traces of catastrophe: A handbook of shock-metamorphic effects in terrestrial meteorite impact structures.* LPI Contribution No. 954. Houston: Lunar and Planetary Institute. 120 p.

Grajales-Nishimura J. M., Cedillo-Pardo E., Rosales-Dominguez C., Moran-Zenteno D. J., Alvarez W., Claeys P., Ruiz-Morales J., Garcia-Hernandez J., Padilla-Avila P., and Sanchez-Rios A. 2000. Chicxulub impact: The origin of reservoir and seal facies in the southeastern Mexico oil fields. *Geology* 28:307–310.

Kastens K. A. and Cita M. B. 1981. Tsunami-induced sediment transport in the abyssal Mediterranean Sea. *Geological Society of America Bulletin* 92:845–857.

Keller G., Stinnesbeck W., Adatte T., Stüben D., and Kramar U. 2003. Chicxulub impact predates K-T boundary: Supports multiple impact hypothesis (abstract). Third International Conference on Large Meteorite Impacts. p. 4020.

Kenkmann T., Wittmann A., Scherler D., and Stöffler D. 2003. The Cretaceous sequence of the Chicxulub Yax-1 drillcore: What is impact-derived? (abstract). Third International Conference on Large Meteorite Impacts. p. 4075.

Kiyokawa S., Tada R., Iturralde-Vinent M. A., Tajika E., Yamamoto S., Oji T., Nakano Y., Goto K., Takayama H., Delgado D. G., Otero C. D., Rojas-Consuegra R., and Matsui T. 2002. Cretaceous-Tertiary boundary sequence in the Cacarajicara formation, western Cuba: An impact-related, high energy, gravity-flow deposit. In *Catastrophic events and mass extinctions: Impact and beyond,* edited by Koeberl C. and Macleod G. Special Paper 356. Boulder: Geological Society of America. pp. 125–144.

Koshikawa T., Kido Y., and Tada R. 2003. High resolution rapid elemental analysis using an XRF micro-scanner. *Journal of Sedimentary Research* 73:824–829.

Lindström M., Floden T., Grahn Y., and Kathol B. 1994. Post-impact deposits in Tvären: A marine Ordovician crater south of Stockholm, Sweden. *Geological Magazine* 131:91–103.

Matsui T., Imamura F., Tajika E., Nakano Y., and Fujisawa Y. 2002. Generation and propagation of a tsunami from the Cretaceous/Tertiary impact event. In *Catastrophic events and mass extinctions: Impact and beyond,* edited by Koeberl C. and Macleod G. Special Paper 356. Boulder: Geological Society of America. pp. 69–77.

Middleton G. V. and Hampton M. A. 1976. Subaqueous sediment transport and deposition by sediment gravity flows. In *Marine sediment transport and environmental management,* edited by Stanley D. J. and Swift D. J. P. New York: Wiley. pp. 197–218.

Middleton G. V. and Southard J. B. 1977. *Mechanics of sediment movement: SEPM lecture notes for short course No. 3.* 401 p.

Morgan J., Warner M., and Chicxulub working group. 1997. Size and morphology of the Chicxulub impact crater. *Nature* 390:472–476.

Morgan J. V., Warner M. R., Collins G., Melosh H. J., Christeson G. L. 2000. Peak-ring formation in large impact craters: Geophysical constraints from Chicxulub. *Earth and Planetary Science Letters* 183:347–354.

Ormö J. 1994. The pre-impact Ordovician stratigraphy of the Tvären Bay impact structure, SE Sweden. *GFF* 116:139–144.

Ormö J. and Lindström M. 2000. When a cosmic impact strikes the sea bed. *Geological Magazine* 137:67–80.

Pierazzo E. and Crawford D. A. 1997. Hydrocode simulations of Chicxulub as an oblique impact event (abstract). Large Meteorite Impacts and Planetary Evolution Conference. p. 40.

Pierazzo E., Kring D. A., and Melosh H. J. 1998. Hydrocode simulation of the Chicxulub impact event and the production of climatically active gases. *Journal of Geophysical Research* 103 28607–28625.

Poag C. W., Powars D. S., Poppe L. J., and Mixon R. B. 1994. Meteoroid mayhem in Ole Virginny: Source of the North American tektite strewn field. *Geology* 22:691–694.

Poag C. W., Plescia J. B., and Molzer P. C. 2002. Ancient impact structures on modern continental shelves: The Chesapeake Bay, Montagnais, and Toms Canyon craters, Atlantic margin of North America. *Deep-Sea Research II* 49:1081–1102.

Sharpton V., Marin L. E., Carney J. L., Lee S., Ryder G., Schuraytz B. C., Sikora P., and Spudis P. D. 1996. A model of the Chicxulub impact basin based on evolution of geophysical data, well logs, and drill core samples. In *Cretaceous-Tertiary event and other catastrophes in Earth history,* edited by Ryder G., Fastovsky D., and Gartner S. Special Paper 307. Boulder: Geological Society of America. pp. 55–74.

Smit J., Roep T. B., Alvarez W., Montanari A., Claeys P., Grajales-Nishimura J. M., and Bermudez J. 1996. Coarse-grained, clastic sandstone complex at the K/T boundary around the Gulf of Mexico: Deposition by tsunami waves induced by the Chicxulub impact? In *Cretaceous-Tertiary event and other catastrophes in Earth history,* edited by Ryder G., Fastovsky D., and Gartner S. Special Paper 307. Boulder: Geological Society of America. pp. 151–182.

Smit J. 1999. The global stratigraphy of the Cretaceous-Tertiary boundary impact ejecta. *Annual Review of Earth and Planetary Sciences* 27:75–113.

Smit J., Dressler B., Buffler R., Moran D., Sharpton B., Stoeffler D., Urrutia J., and Morgan J. 2003. Stratigraphy of the Yaxcopoil-1 drill hole in the Chicxulub impact crater (abstract). EGS-AGU-EUG Joint Assembly. p. 6498.

Tada R., Nakano Y., Iturralde-Vinent M. A., Yamamoto S., Kamata T., Tajika E., Toyoda K., Kiyokawa S., Delgado D. G., Oji T., Goto K., Takayama H., Rojas-Consuegra R., and Matsui T. 2002. Complex tsunami waves suggested by the Cretaceous-Tertiary

boundary deposit at the Moncada section, western Cuba. In *Catastrophic events and mass extinctions: Impact and beyond,* edited by Koeberl C. and Macleod G. Special Paper 356. Boulder: Geological Society of America. pp. 109–123.

Tada R., Iturralde-Vinent M. A., Matsui T., Tajika E., Oji T., Goto K., Nakano Y., Takayama H., Yamamoto S., Rojas-Consuegra R., Kiyokawa S., García-Delgado D., Díaz-Otero C., and Toyoda K. Forthcoming. K/T boundary deposits in the proto-Caribbean basin. *American Association of Petroleum Geologists Memoir.*

Takayama H., Tada R., Matsui T., Iturralde-Vinent M. A., Oji T., Tajika E., Kiyokawa S., Garcia D., Okada H., Hasegawa T., and Toyoda K. 2000. Origin of the Peñalver Formation in northwestern Cuba and its relation to K/T boundary impact event. *Sedimentary Geology* 135:295–320.

Wittmann A., Kenkmann T., Schmitt R. T., Hecht L., and Stöffler D. 2003. Impact melt rocks in the "Cretaceous megablock sequence" of drill core Yaxcopoil-1, Chicxulub crater, Yucatán, Mexico (abstract). Third International Conference on Large Meteorite Impacts. p. 4125.